include: (1) inadequacy in the basis set, (2) a significant difference between the OVD and the MD, (3) instrumental broadening of the experimental density, (4) contamination of the 1e″ density by the 6e′, and (5) the effect of geometric distortion on the momentum density.

In order to test the importance of these possibilities, we have carried out calculations of the 1e″ MD using 3-21G$^+$, 3-21G^{+**}, and 6-311^{+**} bases. The OVD was then explicitly calculated from CI wave functions using a 3-21G$^+$ basis. In order to compare our calculations with observations, the effect of finite angular and energy resolution of the instrument has been simulated using the convolution procedure devised by Bawagan.[10] The momentum scale for the experimental results was adjusted accordingly, and the effects of resolution on the transmission function of the instrument was accounted for by a calibration against argon as explained previously.[11] Initially a geometry optimization was performed on borazine at the SCF 3-21G** level in D_{3h} symmetry using the program GAMESS,[12] obtaining B-N, B-H, and N-H bond distances of 1.429, 1.198, and 0.998 Å, respectively, and a B-N-B angle of 122.3°. These values are in good agreement with electron diffraction results[13] (R(B-N) = 1.435 Å, ∠B-N-B = 122.5°) and with previous calculations.[2] We then added diffuse s- and p-functions on B and N so as to better represent the low-momentum components[14] which are underestimated by split-valence bases.[15] As mentioned above, the momentum density obtained for the 1e″ HOMO of $B_3N_3H_6$ with this 3-21G^{+**} basis set is clearly more localized in momentum space than the experimental result, although its maximum is at about the same position.

We next calculated CI wave functions for neutral $B_3N_3H_6$ and its various cations and used them to evaluate binding energies and OVDs using the program MELD.[16] Due to computer limitations we were forced to employ for the CI calculations only a 3-21G$^+$ basis (e.g., diffuse s- and p-functions, but no polarization functions); however, the spin-coupled calculations,[4] going beyond the SCF model, have yielded similar descriptions of correlation effects using both double-ζ and polarized-triple-ζ bases, so our 3-21G$^+$ basis set should still recover an important fraction of the correlation effects. The 3-21G$^+$ canonical MO is almost indistinguishable from the 3-21G^{+**} result, indicating that polarization functions have little effect upon the momentum densities at the Hartree-Fock level. Freezing the six B1s and N1s core orbitals employing 29 virtual orbitals in the CI and using C_{2v} symmetry, we obtained the binding energies shown in Table I. These are comparable to experimental binding energies[8] as well as those from previous SCF calculations.[9] The calculated molecule-cation OVD for the lowest energy $(1e'')^{-1}$ cation is also shown in Figure 1. Although its amplitude at small momentum is increased somewhat compared to that of the 1e″ CMO, its overall agreement with the experimental result is only slightly improved.

Contributions from the 6e′ orbital, with an experimental binding energy of 11.4 eV, cannot explain the discrepancy between measurement and calculation since our energy resolution is sufficient to all but exclude the contributions from this orbital. In any event, the 6e′ orbital has too little amplitude at momentum values above 1.0 a_0^{-1} to explain the observed amplitude in the high-momentum region.

Calculations indicate that the $(1e'')^{-1}$ cation in $B_3N_3H_6$ shows an appreciable Jahn-Teller distortion.[17] We have previously seen Jahn-Teller effects in the momentum densities of cyclopropane and have analyzed them by considering distortions of the cations;[18] however, using equilibrium geometries for the borazine cations calculated at the SCF 3-21G level (which are almost identical to those previously reported[17]), we find a MD for either component of the 1e″ MO almost identical to that in the neutral molecule. Our CI calculations are certainly limited in scope because of our small basis set and our truncation of the virtual orbital space, but they do yield accurate binding energies (Table I) and give an energy lowering using K orbital virtuals[19] of 0.3175 hartrees compared to the SCF result (almost 10 times larger than that from a full-valence VB calculation[4]). Thus, at least on energetic grounds, the CI calculations are of reasonable accuracy.

Finally, it is worth noting that previous (e,2e) studies of benzene[20] and *p*-dichlorobenzene[21] also showed experimental cross sections systematically broader than those calculated at the double-ζ SCF level. Inclusion of diffuse functions would be expected to move momentum density to lower values of momentum rather than making the distribution of density broader.

We are led to the conclusion that the borazine 1e″ ionization is much more localized in character than theory predicts. To emphasize this conclusion we show in Figure 1 the momentum density calculated at the SCF 3-21G^{+**} level for the N2p electron in ^{4}S atomic nitrogen. The experimental cross-section for the 1e″ orbital resembles that of an isolated N2p orbital more than a (N2p,B2p)-π CMO. Such localization may be present in either the neutral molecule or the cation, or both. Broken-symmetry Hartree-Fock and CI calculations may be needed to describe it correctly.[22]

Acknowledgment. The support of the National Science Foundation (CHE-88-08589) is acknowledged. Professor E. R. Davidson (Indiana University) provided a copy of the MELD program, and Prof. A. O. Bawagan (Carleton University) provided his convolution routine.

(10) Graham, L. A.; Bawagan, A. D. O. *Chem. Phys. Lett.* **1991**, *178*, 441. Bawagan, A. O.; Brion, C. E. *Chem. Phys.* **1990**, *144*, 167.
(11) Gorunganthu, R. R.; Coplan, M. A.; Moore, J. H.; Tossell, J. A. *J. Chem. Phys.* **1988**, *89*, 25.
(12) Schmidt, M. W.; Boatz, J. A.; Baldridge, K. K.; Koseki, S.; Gordon, M. S.; Elbert, S. T.; Lam, B. *QCPE Bull.* **1987**, *7*, 115.
(13) Harshbarger, W.; Lee, G.; Porter, R. F.; Bauer, S. H. *Inorg. Chem.* **1969**, *8*, 1683.
(14) Clark, T.; Chandrasekhar, J.; Spitznagel, G. U.; Schlegel, P. v. R. *J. Comput. Chem.* **1983**, *4*, 294.
(15) Gorunganthu, R. R.; Coplan, M. A.; Leung, K. T.; Tossell, J. A.; Moore, J. H. *J. Chem. Phys.* **1989**, *91*, 1994.
(16) McMurchie, L.; Elbert, S. T.; Langhoff, S. R.; Davidson, E. R. *NRCC Software Catalog*; Vol. 1, QC4 MELD LBL-10811 UC-4, 1980.
(17) Kato, H.; Hirao, K.; Sano, J. *THEOCHEM* **1983**, *104*, 489.
(18) Tossell, J. A.; Moore, J. H.; Coplan, M. A. *Chem. Phys. Lett.* **1979**, *67*, 356.
(19) Feller, D.; Davidson, E. R. *J. Chem. Phys.* **1981**, *74*, 3977.
(20) Fuss, I.; McCarthy, I. E.; Minchinton, A.; Weigold, E.; Larkins, F. P. *Chem. Phys.* **1981**, *63*, 19.
(21) Bawagan, A. O.; Brion, C. E.; Coplan, M. A.; Tossell, J. A.; Moore, J. H. *Chem. Phys.* **1986**, *110*, 153.
(22) Martin, R. L. *J. Chem. Phys.* **1981**, *74*, 1852.

2D ^{13}C-Coupled HMQC-ROESY: A Probe for NOEs between Equivalent Protons

Jun Kawabata,*[1] Eri Fukushi,[2] and Junya Mizutani[1]

Department of Agricultural Chemistry and GC-MS & NMR Laboratory, Faculty of Agriculture Hokkaido University, Sapporo 060, Japan

Received August 19, 1991

There have been an increased number of naturally occurring C_2 symmetric molecules showing biological activities.[3] In the structure determination of such symmetric molecules, some difficulties due to the presence of two equivalent units in a molecule may arise. We have demonstrated methods for the detection of the chemical connectivity between equivalent carbons of a C_2 molecule, hopeaphenol (**1**),[4] from an isotopomeric point of view.[5]

(1) Department of Agricultural Chemistry.
(2) GC-MS & NMR Laboratory.
(3) For examples, see: Hammann, P.; Kretzschmar, G. *Magn. Reson. Chem.* **1991**, *29*, 667-670. Kitagawa, I.; Kobayashi, M.; Katori, T.; Yamashita, M.; Tanaka, J.; Doi, M.; Ishida, T. *J. Am. Chem. Soc.* **1990**, *112*, 3710-3712. Kato, Y.; Fusetani, N.; Matsunaga, S.; Hashimoto, K.; Sakai, R.; Higa, T.; Kashman, Y. *Tetrahedron Lett.* **1987**, *28*, 6225-6228. Nakagawa, M.; Endo, M.; Tanaka, N.; Gen-Pei, L. *Tetrahedron Lett.* **1984**, *25*, 3227-3230.
(4) Coggon, P.; Janes, N. F.; King, F. E.; King, T. J.; Molyneux, R. J.; Morgan, J. W. W.; Sellars, K. *J. Chem. Soc.* **1965**, 406-409.

0002-7863/92/1514-1115$03.00/0

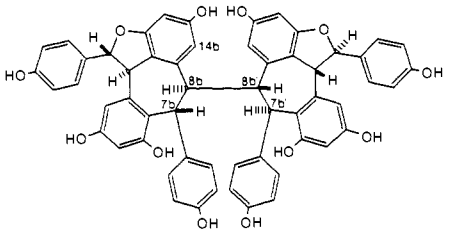

1

In this communication, we apply this concept to the detection of NOEs between equivalent protons which cannot be observed by the conventional NMR methods. The two identical units of **1** are connected with a single C8b–C8b′ bond and the whole molecule has C_2 symmetry, regardless of the angle between two units. Although the relative stereochemistry *within* each unit of **1** has been clarified by X-ray analysis,[6] no information concerning the spatial relationship *between* the two units has been available. During the course of a search for antibacterial oligostilbenes in *Carex* spp. (Cyperaceae),[7] we have isolated **1** from *Carex pumila*.[5] Here, we determine the conformation around the central 8b–8b′ bond by demonstrating the existence of an NOE between 7b-H and 7b′-H.

Discrimination of equivalent protons, e.g., 7b-H/7b′-H of **1**, will be accomplished as ^{12}C-H and ^{13}C-H, since the former is observed as a singlet in the ^{1}H NMR spectrum whereas the latter splits into a doublet by large $^1J_{CH}$. Recently, observation of HOHAHA cross-peaks between overlapped protons by a similar concept using a 2D ^{13}C-coupled HMQC–TOCSY sequence[8] was reported, and the possibility of utilizing HMQC–NOESY for the detection of NOE cross-peaks in such cases was indicated.[8,9] At first, we applied this ^{13}C-coupled HMQC–NOESY sequence[8] to detect an NOE between 7b-H and 7b′-H, which would give evidence for the anti conformation of **1** as mentioned below. The delay time immediately after the BIRD sequence for nulling center signals was carefully optimized and set to 0.4 s, and the mixing time was also 0.4 s. The result obtained (Figure 1A), however, was disappointing in that only a weak positive cross-peak appeared at the center of the positive doublet due to the direct correlation of 7b-H/7b-C. This central in-phase peak is considered to arise from a weak negative NOE between 7b-H and 7b′-H, as these protons are located at the less mobile inner part of this molecule of intermediate size.[10] Thus the spatial proximity of these protons should be detected more efficiently by using a rotating-frame NOE (ROE).[11] The ^{13}C-coupled HMQC–ROESY sequence was then constructed (Figure 2), and the resultant spectrum of the same region as for the NOESY version is shown in Figure 1B. Both the null interval for BIRD and the mixing time were set to 0.4 s. The spin-lock pulse was derived from the high-power output of the decoupler attenuated by 18 dB, and the radio frequency (rf) field strength, γB_2, was 2.5 kHz. The carrier frequency was positioned at 6.7 ppm. A strong ROE-relayed negative cross-peak clearly appeared between the 7b-H/7b-C doublet. Additional ROE correlations for 7b-H/8b-H and 8b-H/14b-H were also detected in the region. This result strongly supported the anti conformation of **1** in which 7b-H is located in close proximity to 7b′-H, as shown in Figure 3.

Detection of an NOE between equivalent protons by a 2D ^{13}C-coupled HMQC–ROESY sequence at natural abundance has thus been achieved. Although a 2D HMQC–ROESY sequence with carbon decoupling was reported by Davis as a variant of its HOHAHA analogue,[13] this is the first example of the application

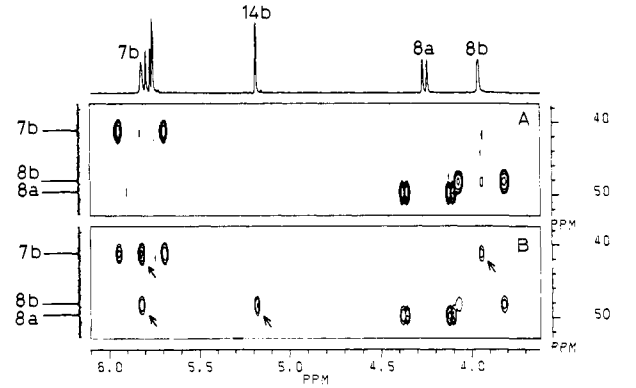

Figure 1. Part of the 2D phase-sensitive ^{13}C-coupled HMQC–NOESY (A) and -ROESY (B) spectra of 50 mg of hopeaphenol (**1**) in acetone-d_6 recorded on a Bruker AM 500 spectrometer (500 MHz). Negative cross-peaks are marked by arrows. The spectra were obtained with the pulse sequences reported by Crouch et al.[8] (A) and shown in Figure 2 (B). The BIRD delay and mixing time for both experiments were 0.4 s. The carrier frequency was positioned at 6.7 ppm, and a 2.5-kHz spin-lock field was used in spectrum B. The spectra were measured covering the spectral width of 3 (A) and 5 (B) kHz in 2K data points using 224 transients for each of 116 t_1 increments. Zero-filling to 0.5K for F_1 and multiplication with squared cosine bell windows in both dimensions were performed prior to 2D Fourier transformation. The total measuring time of each experiment was ca. 21 h.

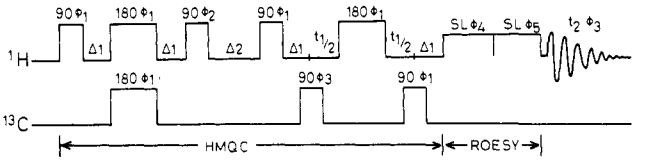

Figure 2. Pulse sequence for the 2D ^{13}C-coupled HMQC–ROESY experiment. Δ_1 is $1/2\,^1J_{CH}$, where Δ_2 is a delay for eliminating ^{12}C-bonded proton signals. ROESY mixing was achieved by a spin lock divided into two parts (shifted in phase by +90° and −90°).[12] TPPI was applied for quadrature detection in F_1. Phase cycling used is as follows: ϕ_1 = $x,-x,y,-y$; ϕ_2 = $-x,x,-y,y$; ϕ_3 = $x,x,y,y,-x,-x,-y,-y$; ϕ_4 = $y,-y,x,-x$; ϕ_5 = $-y,y,-x,x$.

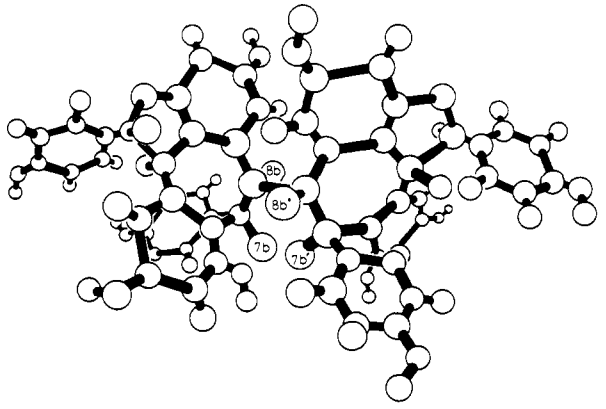

Figure 3. Perspective view of **1**.

(5) Kawabata, J.; Fukushi, E.; Hara, M.; Mizutani, J. *Magn. Reson. Chem.*, in press.

(6) Coggon, P.; King, T. J.; Wallwork, S. C. *Chem. Commun.* **1966**, 439–440.

(7) Suzuki, K.; Shimizu, T.; Kawabata, J.; Mizutani, J. *Agric. Biol. Chem.* **1987**, *51*, 1003–1008. Kawabata, J.; Ichikawa, S.; Kurihara, H.; Mizutani, J. *Tetrahedron Lett.* **1989**, *30*, 3785–3788. Kurihara, H.; Kawabata, J.; Ichikawa, S.; Mizutani, J. *Agric. Biol. Chem.* **1990**, *54*, 1097–1099. Kawabata, J.; Mishima, M.; Kurihara, H.; Mizutani, J. *Phytochemistry* **1991**, *30*, 645–647. Kurihara, H.; Kawabata, J.; Ichikawa, S.; Mishima, M.; Mizutani, J. *Phytochemistry* **1991**, *30*, 649–653.

(8) Crouch, R. C.; McFadyen, R. B.; Daluge, S. M.; Martin, G. E. *Magn. Reson. Chem.* **1990**, *28*, 792–796.

(9) Recently, only one example of this sequence was reported, although no experimental details were mentioned: Martin, G. E.; Crouch, R. C. *J. Nat. Prod.* **1991**, *54*, 1–70.

(10) The similar phenomenon was observed in a carotenoid: Englett, G.; Bjornland, T.; Liaaen-Jensen, S. *Magn. Reson. Chem.* **1990**, *28*, 519–528.

(11) Bothner-By, A. A.; Stephens, R. L.; Lee, J.; Warren, C. D.; Jeanloz, R. W. *J. Am. Chem. Soc.* **1984**, *106*, 811–813. Bax, A.; Davis, D. G. *J. Magn. Reson.* **1985**, *63*, 207–213.

(12) Neuhaus, D.; Keeler, J. *J. Magn. Reson.* **1986**, *68*, 568–574.

(13) Davis, D. G. *J. Magn. Reson.* **1989**, *84*, 417–424.

of the ^{13}C-coupled sequence to the structural analysis of the C_2 symmetric molecule.

Acknowledgment. This work was supported in part by a Grant-in-Aid for Scientific Research (No. 03760075 to J.K.) from the Ministry of Education, Science and Culture of Japan.

Sequential Binding of Aluminum(3+) to the C- and N-Lobes of Human Serum Transferrin Detected by ^1H NMR Spectroscopy

Gina Kubal and Peter J. Sadler*

Department of Chemistry, Birkbeck College
University of London
Gordon House and Christopher Ingold Laboratory
29 Gordon Square, London WC1H 0PP, U.K.

Robert W. Evans

Department of Biochemistry, UMDS
Guy's Hospital Medical School
St. Thomas Street, London SE1 9RT, U.K.

Received May 30, 1991

The deposition of Al^{3+} in the brain is known to cause dialysis encephalopathy and may also be involved in other conditions of medical concern.[1] The major transport agent for Al^{3+} in the body is thought to be the Fe-binding protein transferrin,[2,3] and much attention is now focused on the design of chelating agents to remove Al^{3+} from this protein. Recent UV data[3] show that Al^{3+} binds strongly to the specific Fe^{3+} sites of human serum transferrin (HTF) with log K values of 13.5 (C-lobe) and 12.5 (N-lobe). Direct methods for detecting the binding of Al^{3+} to the individual lobes of intact HTF in solution are required. In the only previous high-resolution ^1H NMR study of HTF,[4] it was noted that the resolution and sensitivity did not allow the analysis of individual resonances, as might be expected for such a high M_r protein (79 kDa). We show here[5] that many individual resonances can be resolved in resolution-enhanced 500-MHz ^1H NMR spectra of intact HTF. This allows the study of sequential loading of Al^{3+} into the C- and N-lobes, Al^{3+}-induced structural changes in the protein, and the monitoring of Al^{3+} removal by therapeutic chelating agents.

Many resonances are resolved in both the aliphatic and aromatic regions of 500-MHz ^1H NMR spectra of apo-HTF,[6,7] when enhanced by combined application of exponential and sine-bell functions to the free induction decay, as shown in Figure 1. This procedure[8] removes broad resonances from the spectrum, leaving sharp peaks from protons in the most mobile regions of the protein. The most intense peaks, ca. 2.1 and 3.4–4 ppm (not shown), arise from glycan *N*-acetyl and sugar ring protons, respectively, in two biantennary chains in the C-lobe. High-field-shifted resonances (ca. 0.6 to −0.7 ppm), which are likely to arise from methyls close to the faces of aromatic side chains, are clearly visible, and in the aromatic region about six peaks assignable to His C2H protons can be seen.[9] Peaks for the majority of amino acids are absent from enhanced spectra because they are very broad, which may be related to the immobility of many regions of the apoprotein.

The effect of Al^{3+} addition to HTF[10] is shown in Figure 1. In the high-field methyl region, new peaks a and e appear after addition of 1 molar equiv of Al^{3+}, but these are little affected by further addition of Al^{3+}, whereas peak d disappears progressively. Peaks in the Lys/Arg $\epsilon/\delta CH_2$ region, ca. 3 ppm,[11] also disappear in the presence of Al^{3+}, but the sugar peaks are unaffected. In the His C2H region, new resonances such as h, o, and q appear on addition of Al^{3+}, increase in intensity until 1 equiv has been added, and change little on further addition, whereas peaks r and l disappear and appear, respectively, on addition of the second equivalent of Al^{3+}; see inset in Figure 1B. Peaks such as p (apparently a single His C2H on pH* titration) and d change their intensities on binding both the first and second equivalents of Al^{3+}. Other specific changes are notable in the region 6.2–7.4 ppm of the aromatic region involving His C4H peaks and perhaps other aromatic residues.

Thus Al^{3+} binding to intact HTF can be detected by ^1H NMR spectroscopy, and the data suggest that sequential binding of Al^{3+} to the C- and N-lobes of HTF can be followed together with Al^{3+}-induced structural changes. With the assumption that Al^{3+} binds more strongly to the C-lobe,[3] peaks h, o, and q can be tentatively assigned to His residues in the C-lobe, and peaks l and r to the N-lobe, although the possibility that binding to one lobe affects resonances of the other cannot be ruled out. Several peaks appear to be sensitive to the occupation of both lobes, and this may indicate that Al^{3+} binding involves interlobal communication. Peaks for >10 His residues appear to be seen in spectra of Al_2-HTF, but it is not clear yet whether these include His-249 and His-585 (Fe^{3+} ligands);[2] Al^{3+} would be expected to have a lower affinity for N ligands than Fe^{3+}. The changes in shift of high-field methyl groups imply that Al^{3+} binding affects the

* Author to whom correspondence should be addressed.

(1) Articles in the following: *Met. Ions Biol. Syst.* **1988**, 24.

(2) HTF:678 amino acids in two structurally homologous but chemically distinct lobes; two domains in each lobe form the Fe-binding clefts with two Tyr, one His, one Asp, and CO_3^{2-} as ligands. Lys and/or Arg residues may stabilize bound CO_3^{2-}. The crystal structure of HTF has not been reported. X-ray structure of rabbit serum transferrin: Bailey, S.; Evans, R. W.; Garratt, R. C.; Gorinsky, B.; Hasnain, S.; Horsburgh, C.; Jhoti, H.; Lindley, P. F.; Mydin, A.; Sarra, R.; Watson, J. L. *Biochemistry* **1988**, *27*, 5804–5812. Related proteins: melanotransferrin, ovotransferrin, and lactotransferrin. See: Baker, E.; Rumball, S. V.; Anderson, B. F. *Trends Biochem. Sci.* **1987**, *12*, 350–353. Crichton, R. C. *Adv. Protein Chem.* **1990**, *40*, 281–363.

(3) Harris, W. R.; Sheldon, J. *Inorg. Chem.* **1990**, *29*, 119–124 and references therein.

(4) Woodworth, R. C.; Williams, R. J. P.; Alsaadi, B. M. In *Proteins of Iron Metabolism*; Brown, E. B., Aisen, P., Fielding, J., Crichton, R. R., Eds.; Grune and Stratton: New York, 1977; p 211. Better resolution has been obtained from the N-lobe, and the effect of pH and Ga^{3+} on the His C2H peaks has been reported: Valcour, A. A.; Woodworth, R. C. *Biochemistry* **1987**, *26*, 3120–3125. However, it is also important to study intact transferrin because there is thought to be a functionally-significant association between the N- and C-lobes in solution: Brown-Mason, A.; Brown, S. A.; Butcher, N. D.; Woodworth, R. C. *Biochem. J.* **1987**, *245*, 103–109.

(5) Presented in part at ICBIC-5, Oxford, August 1991: Bell, J. D.; Evans, R. W.; Kiang, W.; Kubal, G.; Radulovic, S.; Sadler, P. J.; Williams, G. *J. Inorg. Biochem.* **1991**, *43*, 488.

(6) Apo-HTF was purchased from Sigma (Catalog No. T0519, Batch 67F9454). Batches sometimes contain bound citrate (Evans, R. W.; Kubal, G.; Sadler, P. J.; Williams, G., unpublished), and these were avoided for Al^{3+} work. Protein concentrations were determined from ϵ_{280} (Luk, C. K. *Biochemistry* **1971**, *10*, 2838–2843). The pH* values of NMR solutions were strictly monitored before and after NMR runs. Control of pH* with bicarbonate buffers is difficult, and pH* 8.78 was chosen to minimize problems from shifts of His peaks which occur at lower pH* values with slight pH* drift. pH* is the pH meter reading in D_2O solutions.

(7) ^1H NMR spectra (500 MHz) were recorded on Bruker AM500 and JEOL GSX500 spectrometers, typically using 0.55 mL in a 5-mm tube, 310 K, 512–650 transients, 45° pulses, relaxation delay 1.5–2 s, 8k data points (zero-filled to 16k), and gated secondary irradiation of HOD. FIDs were processed using exponential functions equivalent to line-broadenings of 1–3 Hz combined with unshifted sine-bell functions.

(8) Sadler, P. J.; Tucker, A. *Biochem. Soc. Trans.* **1990**, *18*, 923–924.

(9) Assignments of His C2H and C4H peaks of apo-HTF have been confirmed by pH titrations (Kubal, G.; Sadler, P. J., unpublished). Over the range pH* 3–11, titration curves for ca. 14 His C2H peaks can be followed (i.e., several His C2H peaks overlap at pH* 8.78). There are 19 His residues in HTF; 10 in the C-lobe and nine in the N-lobe. Sugar protons are seen clearly in 2D COSY spectra, together with cross peaks for several amino acid residues.

(10) Added as microliter aliquots of a stock solution of $Al_2(SO_4)_3 \cdot 16H_2O$ (BDH) in D_2O (pH* 3.4). UV spectra of similar HTF solutions (after 50× dilution in the same buffer) were also recorded. New maxima were observed at 240 and 288 nm for Al-HTF with intensities similar to those reported,[3] and characteristic of coordinated tyrosines, showing that Al^{3+} binds to the high-affinity metal sites under our conditions.

(11) Wüthrich, K. *NMR of Proteins and Nucleic Acids*; Wiley: New York, 1986.

0002-7863/92/1514-1117$03.00/0